12-1-2006

Reliability-based Optimization of Fiber-reinforced Polymer Composite Bridge Deck Panels

Michel D. Thompson
Mississippi State University, Starkville, MS

Christopher D. Eamon
Mississippi State University, Starkville, MS, christopher.eamon@wayne.edu

Masoud Rais-Rohani
Mississippi State University, Starkville, MS

Reliability-Based Optimization of Fiber-Reinforced Polymer Composite Bridge Deck Panels

Michel D. Thompson[1], Christopher D. Eamon[2], and Masoud Rais-Rohani[3]

Manuscript # ST/2005/024585

Database Headings: structural reliability, optimization, composite materials, bridges, bridge decks

Abstract

A reliability-based optimization (RBO) procedure is developed and applied to minimize the weight of eight fiber-reinforced polymer composite bridge deck panel configurations. The method utilizes interlinked finite element, optimization, and reliability analysis procedures to solve the weight minimization problem with a deterministic strength constraint and two probabilistic deflection constraints. Panels are composed of an upper face plate, lower face plate, and a grid of interior stiffeners. Different panel depths and stiffener layouts are considered. Sensitivity analyses are conducted to identify significant design and random variables. Optimization design variables are panel component ply thicknesses while random variables include load and material resistance parameters. It was found that panels were deflection-governed, with the optimization algorithm yielding little improvement for shallow panels, but significant weight savings for deeper panels. The best design resulted in deep panels with close stiffener spacing to minimize local upper face plate deformations under the imposed traffic (wheel) loads.

---

[1]Former graduate student, Mississippi State University, Dept of Civil Engineering. Mississippi State, MS 39762
[2]Assistant Professor, Mississippi State University, Dept. of Civil Engineering. Email: eamon@engr.msstate.edu
[3]Professor, Mississippi State University, Dept. of Aerospace Engineering. Email: masoud@ae.msstate.edu

Introduction

For most of the state, county, and city bridges that are defined as deficient or functionally obsolete by the Federal Highway Administration, replacement of the existing deteriorated deck (usually reinforced concrete) would return the bridge to a structurally sound condition (Zureick, et al., 1995). Other bridges have deficiencies in the substructure that require a reduction in allowed live (traffic) load. Both of these problems may be addressed with the use of a lightweight composite modular deck to replace the existing deteriorated reinforced concrete deck. To maximize the efficient use of composites, where overdesign is often significantly more costly than traditional civil engineering materials, performing a formal structural optimization to minimize material usage may be beneficial.

As structural safety is most consistently measured probabilistically rather than deterministically, it is appropriate to formulate structural optimization problems based on reliability constraints where safety is a concern. This becomes particularly important when relatively new civil engineering materials such as composites are considered.

In the last two decades, fiber-reinforced polymer (FRP) composite materials have been utilized in the design of lightweight modular deck panels (Mertz, et al., 2003). Previous research considered the reliability-based optimization of FRP composite structures (Antonio, et al., 1993; Yang and Ma, 1990; Liu and Mahadevan, 1996; Frangopol, 1997; Miki, et al., 1997; Deo and Rais-Rohani, 1999; Richard and Perreux, 2000; Conceicao Antonio, 2001; Rais-Rohani and Singh, 2004; Kogiso and Nakagawa, 2003), as well as the design and application of FRP composite materials to bridge decks (Feng and Song, 1990; Henry, 1985; Bakeri, 1989; Bakeri and Sunder, 1990; Plecknik, et al., 1990; Zureick, et al., 1995; Lopez-Anido, et al., 1997;

Williams, et al., 2003). Moreover, traditional deterministic optimization methods have been applied specifically to composite bridge decks in earlier research (McGhee, et al. 1991; Zureick, 1997; He and Aref, 2003). However, there has not been an emphasis placed on the role of uncertainties associated with the material properties, structural dimensions, or applied loads during the optimization. That is, a literature search revealed no studies focused on the reliability-based optimization (RBO) of FRP bridge decks. Therefore, this research attempts to fill this gap by: 1) formulating the proper reliability and deterministic constraint set for an FRP bridge deck; 2) establishing the underlying computational relationships, and; 3) solving the resulting optimization problem by integrating off-the-shelf analysis tools in design optimization, finite elements, and structural reliability.

RBO Problem Formulation

The design optimization problem considered in this research is that of the weight minimization of a modular composite bridge deck panel with deflection and stress (Tsai-Wu failure index) constraints. The RBO problem for a bridge deck panel can be described mathematically as a search for the optimum values of design variables that would minimize bridge deck panel weight subject to constraints on reliability and stress, and is formulated as

$$\text{Min } f = (A_s(16t_{UF} + 8t_{LF}) + 32A_{st}\, n_{SID}\, (t_{TS} + t_{LS}))\, \rho_{comp} \qquad (1)$$

$$\text{s.t.} \quad TW_{max} - 1 \le 0 \qquad (2)$$

$$1 - \beta_d / \beta_{min} \le 0 \qquad (3)$$

$$t_i^L \le t_i \le t_i^U \qquad (4)$$

where A_s and A_{st} are the areas of the panel surfaces (upper and lower) and the stiffeners, respectively; n_{SID} is the number of stiffeners in either the transverse or longitudinal direction; t_{UF},

t_{LF}, t_{TS}, t_{LS} are the mean ply thicknesses for the upper face plate, lower face plate, transverse stiffeners, and longitudinal stiffeners, respectively; ρ_{comp} is the density of the composite material; TW_{max} is the maximum Tsai-Wu failure index in the bridge deck panel; β_d is the calculated reliability index for maximum bridge deck panel deflection, and β_{min} is the minimum acceptable reliability index (note that the constants 8, 16, and 32 in eq. 1 refer to the total number of plies in the lower face plate, upper face plate, and stiffeners, respectively). A more detailed description of the panel is given below under *Bridge Decks Considered,* while a discussion of the choice of deflection for the reliability constraint is given in *RBO Results and Discussion*. The upper and lower bounds t_i^U and t_i^L on the design variables refer to the mean ply thicknesses. The panel configuration is governed by four such design variables, one each for the upper face plate (t_{UF}), the lower face plate (t_{LF}), the group of longitudinal stiffeners (t_{TS}), and the group of transverse stiffeners (t_{LS}) . Bounds for all DVs are t_i^U = 0.635 cm and t_i^L = 0.0025 cm.

The Tsai-Wu failure criterion is used to characterize ply failure in each composite member of the bridge deck. Using this criterion, a ply in a multi-layer laminate is considered failed if

$$(f_1\sigma_1 + f_2\sigma_2 + f_{11}\sigma_1^2 + f_{22}\sigma_2^2 + f_{66}\tau_{12}^2 + 2f_{12}\sigma_1\sigma_2) > 1 \qquad (5)$$

where σ_1, σ_2, and τ_{12} represent the normal ply stress in the longitudinal direction, normal ply stress in the transverse direction, and in-plane shear stress, respectively, with the coefficients defined in terms of normal and shear ply strengths as: $f_1 = 1/X_T - 1/X_C$; $f_2 = 1/Y_T - 1/Y_C$; $f_{11} = 1/(X_T X_C)$; $f_{22} = 1/(Y_T Y_C)$; $f_{66} = 1/S^2$; $f_{12} = -1/(2X_T^2)$. Here X_T and X_C correspond to the ply's tensile and compressive strength in the longitudinal direction, Y_T and Y_C correspond to tensile and compressive strength in the transverse direction, and S is the in-plane shear strength (Jones,

1999). Statistical properties for strength and other material properties for the glass/epoxy composite are given in Table 1 (MIL-17, 1999).

The mathematical programming techniques that are typically used to solve a nonlinear, constrained optimization problem, such as the one defined by Equations (1) through (4), require gradients of the objective function and those of the constraints with respect to each design variable in the form $\partial F_j / \partial X_i$ and $\partial g_j / \partial X_i$. When the objective function and/or constraints are implicit functions of design variables, such as in this study, the derivatives above are calculated using a finite difference scheme, which can significantly increase the computational cost. In this research, the modified method of feasible directions (MMFD) is used to solve the nonlinear programming problem, as described by Vanderplaats (1983).

RBO Computational Framework

A framework is developed to facilitate the integration of various computational tools and to manage the interactions between optimization-directed probabilistic and finite element responses. The system is designed to allow the use of off-the-shelf codes. For the specific RBO problem considered in this study, VisualDOC (VisualDOC, 2002) is used to formulate and solve the design optimization problem as well as to manage the flow of information from one tool to another, PATRAN (MSC/PATRAN, 1998) for finite element modeling, NASTRAN (MSC/NASTRAN, 1998) for finite element analysis (FEA), and NESSUS (Riha, et al., 1999) for structural reliability analysis, although other codes and algorithms can easily be substituted. The steps in a typical RBO cycle is as follows:

1. *Initialize/update design variables:* At the start of the first optimization cycle, the design variables (DVs) have the initial values set by the analyst. In the second and all subsequent cycles, the values are updated based on the optimization results. DVs were allowed to be

incremented up to 0.10 of their previous values by the optimizer. The design variable values are used as inputs for the FEA.

2. *Perform FEA:* A structural analysis is performed and the nodal deflections as well as elemental Tsai-Wu failure indices are recorded.
3. *Search for critical responses:* The maximum nodal deflections and Tsai-Wu failure indices, needed for the reliability analysis as well as the constraint calculations, are extracted from the FEA output file and recorded.
4. *Evaluate standard deviations:* The values of the design variables represent the mean values of thickness random variables. Together with the specified coefficients of variation (COV), the corresponding standard deviations are calculated. These random variable statistical parameters are then passed as input to the structural reliability analysis (SRA).
5. *Perform SRA:* Based on the formulation of the limit state function for deflection and the statistical data on all random variables (including the design variables), the reliability index of the structure is calculated. For these calculations, the derivatives of the limit state with respect to each random variable are necessary. As the limit state is an implicit function of random variables, a forward finite-difference scheme for numerical approximation of the required derivatives is used, which in-turn requires a new FEA solution for each random variable perturbation. All intermediate files containing reliability calculations are purged, and the resulting reliability index is passed on for the evaluation of reliability constraint.
6. *Evaluate design constraints:* All ply failure constraints based on Tsai-Wu failure indices and the deflection constraint based on corresponding reliability index are evaluated and checked for design feasibility as the objective function is minimized. Because the optimization algorithm is based on a gradient search technique, the derivatives of all active and violated

constraints in addition to those of the objective function are necessary. These derivatives are also evaluated using a finite difference scheme. In this study, a constraint is considered active if its value is less than or equal to 0.05.

7. *Check convergence:* Return to step 1 until convergence is reached and the optimum solution is found. Convergence is assumed when changes in objective function are less than 0.001.

Bridge Decks Considered

Two common characteristics of fiber-reinforced polymer (FRP) composite bridge deck panels are modularization for ease of transport and installation, and the use of readily available materials such as glass fibers and epoxy matrix (Mertz, et al., 2003). Also, a modern trend in girder bridge design is to use a wider girder spacing. Therefore, the panel concepts considered in this study are compatible with a 2.44 m (8') girder spacing with overall dimensions of 2.44 m x 2.44 m (8 ft x 8 ft) square. Each square panel is designed to span in both directions and is simply supported on all edges by longitudinal and transverse bridge girders as shown in Figure 1. These support conditions are consistent with those used in existing applications (Gillespie, et al., 2000; Stoll, et al., 2002; GangaRao, et al., 2001).

The bridge deck panels consist of four component groups: an upper face plate, a lower face plate, and longitudinal and transverse stiffeners placed between the two plates. It is assumed that the face plates and stiffeners are manufactured separately and bonded together to form the panel. There are four different stiffener spacings (layouts) at two stiffener depths per layout resulting in a total of eight panel concepts. The four stiffener spacings considered are 0.0677 m (2.667 in), 0.1355 m (5.334 in), 0.2032 m (8 in), and 0.4064 m (16 in) on center, in both the longitudinal and transverse directions. The panel concepts with "shallow" stiffener depth (i.e., 114 mm (4.5")) are designated as design concepts S3, S5, S8, and S16, whereas the

corresponding concepts with "deep" stiffeners are designated as SD3 (depth = 178 mm (7.0")), SD5 (depth = 190 mm (7.5")), SD8 (depth = 203 mm (8")), and SD16 (depth = 241 mm (9.5")). The variation in stiffener spacings results in thirty-seven stiffeners in each direction for S3/SD3, nineteen stiffeners in each direction for S5/SD5, thirteen stiffeners in each direction for S8/SD8, and seven stiffeners in each direction for S16/SD16. The initial values for each component thickness and the resulting panel weights are given in Tables 3 and 5. These values, along with variation in panel depths, were chosen such that, in addition to just meeting the strength requirements, the flexural stiffnesses of all panel concepts were approximately equal.

Each panel is made of a glass/epoxy (S2-449 43.5k/SP 381 unidirectional tape) material with properties given in Table 3 (*MIL-17,* 1999). Based on recommendations on ply lay-up design (Bakeri, 1989 and Mertz, et al., 2003), three different ply lay-ups are considered: 16 plies in the upper face plate with an initial ply pattern of $[0_2, +45_2, 90_2, -45_2]_S$; 32 plies in the transverse and longitudinal stiffeners with an initial ply pattern of $[0_4, +45_4, 90_4, -45_4]_S$; and 8 plies in the lower face plate with an initial ply pattern of $[0, +45, 90, -45]_S$. In standard ply-pattern notation $[\theta_i, \theta_j \ldots]$, θ refers to the layer orientation angle in degrees, whereas the subscript refers to the number of plies in each ply group, and the subscript "s" refers to a symmetric lay-up where the bracketed group represents half of the total plies in the laminate.

For panel design, the AASHTO HL-93 (AASHTO 2004) design load is applied on the deck surface. For each panel, in one case the design load is applied to maximize deflection, and in a second case to maximize Tsai-Wu failure index (see Figure 2). A more detailed description of the critical deflection and stress locations for each panel is described in the *RBO Results and Discussion* section. The AASHTO design load consists of pressure patches applied over 25 x 50 cm (10 x 20 in) wheel contact areas, resulting in 1351 kPa (196 psi) loads for strength-based

limit states and 772 KPa (112 psi) loads for serviceability (deflection) limit states. The governing wheel load pattern is that of two trucks side-by-side in adjacent lanes; the two wheels in Figure 2 refer to the tires of adjacent vehicles. Panels were designed to just satisfy AASHTO Code strength requirements in addition to a deflection criterion of L/360. Although the current AASHTO LRFD Code has no required composite deck deflection criteria, many practical applications of FRP decks have been voluntarily limited to L/360 or L/300 (Zureick, et al., 1995; GangaRao, et al., 2001; Aref, et al., 1999; Mosallam, et al., 2002; Williams, et al., 2003; Kumar et al., 2004). Therefore, in addition to material strength limits, the serviceability limit of L/360 was imposed. Panel stiffeners were also checked for stability requirements (buckling).

Finite Element Model

The finite element (FE) method is used to model the bridge deck panels for the reliability-based optimization. The FE model of the deck panel consists of 4-node plate elements for the upper face plate, the lower face plate, and the stiffeners (CQUAD4 elements in NASTRAN). A composite ply property model is used that allows detailed description of the composite lay-up, including ply thickness and ply angle orientation, and the calculation of the Tsai-Wu failure criterion. Accounting for these individual layer properties, the appropriate stiffness matrix for the element is generated, as well as layer-specific Tsai-Wu failure index output. FE models ranged from approximately 11,000 elements (30,000 DOF) for SD3 to 4000 elements (20,000 DOF) for S7, with a typical element size throughout all models of approximately 67.7 mm x 67.7 mm (2.667 in x 2.667 in). Increasing mesh density increased the computation time but did not significantly change displacements or ply failure index (TW) values. An example model is shown in Figure 3. The composite materials used for this study

exhibit low ductility, with essentially linear-elastic response until failure. Therefore, the analysis is linear elastic and failure is assumed to occur when the Tsai-Wu index reaches unity. To check panel stability, an Euler buckling analysis was conducted, with eigenvalues and buckling modes extracted using an Inverse Power method.

Reliability Model

The live load (traffic) model is taken from Nowak (1999), and is based on that used to calibrate the AASHTO LRFD Code. The model considers load data from a survey of heavily-loaded trucks on Michigan highways, and includes the probabilities of simultaneous occurrence (trucks side-by-side) as well as multiple presence (multiple trucks in a single lane). The maximum 75-year wheel live load is found to be 97.1 kN (21.83 kips) with a COV of 13%. Impact load is an additional random variable (RV) and is taken as 10% of the live load with COV of 80%, based on field measurements (Nowak and Kim 1998; Nowak et al. 1999). Live load and impact load are lognormally distributed. As dead load is an insignificant portion of the load effect on the panel (less than 1%), it is not considered further in the reliability analysis.

Material properties E_1, E_2, and G_{12} are taken as RVs for each of the four component groups (top face plate, bottom face plate, longitudinal stiffeners, transverse stiffeners). Additional random variables are the component ply thicknesses, with mean values treated as the optimization design variable values. Hence, each panel has four design variables and 18 random variables. No additional random variation is included for the analysis method itself (FEA calculation of deflection and TW failure index). RV statistical parameters are taken from the available literature and are given in Table 4 (Su, et al.2002; *MIL-17*, 1999; Nowak, 1999). To study the effect of distribution type, random variables E_1, E_2, and G_{12} were initially taken as

Weibull, then the reliability analyses were repeated using normal distributions. It was found that results were insensitive to distribution type for these particular RVs.

The probabilistic limit states considered are deflection (g_d) and strength (g_s). For deflection, two reliability indices are computed, one for a deflection limit of L/360 and another for L/180. The limit states are in the form

$$g_d = L/k - \Delta_{\max} \tag{6}$$

$$g_s = 1 - TW_{\max} \tag{7}$$

where k is the deflection limit constant taken as either 180 or 360; L is the panel span (2440 mm); Δ_{max} is the maximum deflection of the panel under the live load model (described above); and TW_{max} is the maximum Tsai-Wu failure index in the panel. Note that Δ_{max} and TW_{max} are evaluated by calls to the FEA code, and thus these values are implicit functions of the load and resistance random variables. As mentioned above, the L/360 limit is based on existing composite deck designs, as the current AASHTO Code has no deflection criteria specified for composite decks. For comparison, the Code does specify a L/300 plate surface deflection limit for steel orthotropic decks. The L/180 limit is provided for comparison and verification of the numerical procedure, but is not practical for construction as quick deterioration of the wearing surface would likely result.

The iterative Advanced Mean Value (AMV+) method is used to calculate reliability index. An expansion of the Rackwitz-Fiessler procedure (Rackwitz and Fiessler 1978), AMV+ typically requires more samples but yields better accuracy for nonlinear functions. The method is described in detail by Wu et al. (1990). For the problems considered in this study, no more than several iterations were required. Once reliability index β is determined, if desired, failure

probability P_f can be approximated with the well-known transformation $P_f = \Phi(-\beta)$, where Φ is the cumulative distribution function of a standard normal random variable.

Reliability Calibration

Using the AMV+ method, reliability indices for the strength and deflection limit states were numerically calculated for each of the eight traditionally-designed panel concepts. Reliability index for the L/180 deflection limit varied from approximately 4.5 (SD3) to 4.7 (S5), and for the L/360 limit varied from approximately -0.42 (S3) to -0.55 (S8 and SD3), and indices for strength varied from approximately 3.4 (deep panels) to greater than 10 (shallow panels). Results are given in Table 4 for all shallow and one deep panel (SD3) concepts. As will be discussed in the next section, the three other deep panels were found to be invalid during the optimization process and were thus removed from further consideration. Below are some observations on the results.

- The L/360 deflection limit governed the deterministic designs. For most panels, satisfying this limit overshadowed the ply strength requirements imposed by the Tsai-Wu failure criterion. This is clear by the large differences in beta values (Table 5) from the L/360 deflection and strength limit states. Strength beta values for all valid panels except SD3 were slightly over 10. Exact values are not given in the table as the numerical algorithm used to compute reliability index begins to lose accuracy for beta values this high. The strength beta value is decreased substantially for the deep-panel design (SD3), which has a substantially greater stiffness-to-strength ratio than its shallow-panel counterparts.
- Although the negative reliability index for L/360 deflection appears unusual, it should be noted that this deflection limit is arbitrarily chosen, while the negative value indicates that there is a significant probability (approximately 70%) that the panel will exceed this

deflection at least once in its assumed 75 year service life. Given the high strength-to-stiffness ratio of composite materials (as well as these particular panel designs) compared to traditional civil engineering materials, this result is understandable. It may also suggest that, as the L/360 limit is often voluntary chosen for composite deck design, the current AASHTO LRFD code may benefit from a reliability-based calibration for a deflection limit state to complement its current strength-based calibration. Here, a revised service load factor might be chosen that would place currently allowed composite design practices into the range of positive deflection reliability. This exploration is beyond the scope of this study.

From these results, the following indices were initially chosen as the target beta constraints β_{min} to be imposed in the reliability-based optimization (in eq 3): 3.0 for strength (the typical reliability index if the deflection limit is removed and designs are based on strength only), 4.6 for L/180 deflection, and -0.50 for L/360 deflection.

RBO Results and Discussion

In solving the RBO problem, the computational effort required to impose multiple probabilistic constraints was found to be prohibitively expensive. Based on initial results, and as expected from the results of the calibration, it was determined that the reliability constraint for deflection limit was significantly more critical than that based on strength limit. Therefore, the strength-based limit was converted to a less-costly deterministic constraint (eq. 2), while the deflection limit was kept as a probabilistic constraint (eq. 3). Two sets of RBO analyses were conducted: one with the deterministic strength constraint and the probabilistic deflection limit of β=4.6 (for L/180), and another with the deterministic strength constraint and the probabilistic

deflection limit of β=-0.5 (for L/360). As the current AASHTO Code is strength- and not deflection-calibrated, treating the strength constraint as deterministic appears to be the most rational choice. Final results were checked to verify this assumption, as discussed below.

Due to the difficulty of satisfying the deflection reliability constraint, the optimized designs for the shallow panels had minimal weight savings (approximately 1 to 5%) over the initial models. In contrast, significant weight savings were obtained for the deep panels (20-55%). Of course, as the final weight savings depends on the efficiency of the initial design, it is apparent that it was much less clear for the authors how to optimally proportion component thicknesses in the deep panels as opposed to the shallow designs.

The initial and optimal weights for all eight panels are shown in Figure 4. As expected, deeper panels are lightest. Another clear trend emerges that indicates smaller stiffener spacing is potentially most efficient. This is because as stiffener spacing increases, the probabilistic deflection constraint requires a thicker deck surface to limit local deflection, or 'dimpling', under the wheel load between adjacent stiffeners.

As the optimizer may decrease the thickness of the deck stiffeners, local buckling may become a concern. Initial studies revealed that including a buckling constraint in the optimization process would increase the computational cost to the point of infeasibility, so buckling was not included as a constraint. To insure adequate stability, however, all panels were checked for stiffener buckling as part of the post-optimization evaluation. An examination of the models revealed that SD5, SD8, and SD16 had webs that did not meet buckling requirements. Increasing the web thickness of these panels to satisfy buckling requirements still resulted in designs that were lighter than the initial shallow panels. However, the best optimized design, SD3, met buckling requirements and was lighter than the remaining panels, even before the web

thicknesses of these panels were increased, as indicated in Figure 4. Thus, including a buckling constraint in the optimization would not have changed the conclusion that panel SD3 was the most efficient design.

Specific results for the panels that met the stability requirements are given in Table 5. An interesting trend appears with regard to the individual component weights. Referring to Table 5, the upper deck surface in most optimal panel concepts has roughly twice the weight of the stiffeners as well as the lower deck surface. In the least efficient design, S16, the upper deck surface is roughly three times the weight of the stiffeners and of the lower deck surface. However, in the most efficient design, SD3, the weight of the stiffener group is roughly equal to the weight of the upper deck surface. Thus, the most efficient design (SD3) has the largest proportion of material in the stiffeners, while the least efficient design (S16) has the largest proportion of material in the upper deck surface. The reason for this result is the probabilistic deflection limit, which for the inefficient designs with widely-spaced stiffeners, is not governed by the overall panel deflection (spanning from its supports), but rather by local deflection of the upper deck surface of the panel between stiffeners. Comparing S3 to SD3, for the same stiffener spacing, the added depth results in an overall lighter section, even though proportionally more material is needed near the middle of the panel to increase stiffener depth. Removing the deflection limit state and basing designs on solely on strength may of course produce significantly different optimization results.

All optimized structures met the target reliability limits for deflection and the deterministic strength limit. As previously determined, a Tsai-Wu index equal to 1.0 (indicating failure) is associated with a strength reliability index of approximately 3.0 for these particular panels. The strength constraint was inactive (i.e., below an index of 0.95) for all panels.

Note that for all the results, only one set of final values is presented for both probabilistic deflection limits L/180 and L/360. This is because it was found that the end results of both cases are essentially identical. The reason for this is that, as long as the deflection limit is active and driving the optimization process over that of the other constraints, such as strength, then the final results should converge to the same solution, regardless of how 'strict' the imposed probabilistic limit. However, if a less strict reliability index constraint were chosen for deflection that allowed the strength constraint to have a greater impact, then potentially very different results would be obtained, as the strength constraint might now drive the design. However, as such choices do not correspond to reliability levels associated with current design practice, they were deemed impractical and not considered in this study.

Figure 5 shows the design iteration history for the objective function (weight) for each model. In general, convergence was stable and monotonic. Table 6 gives information on computational requirements for each RBO problem. Figure 6 shows the design variable iteration history for the most efficient panel, SD3. Design variable history plots of the other panels (S3, S5, S8, S16) revealed little changes, as the as-designed component thicknesses were already close to optimum values, as discussed below. A check was made to insure that the load positions that caused maximum values of deflection and Tsai-Wu failure index did not change during the optimization (see Figure 2). This is important to verify as load position was kept constant throughout the optimization process. Furthermore, to check the sensitivity of the optimization results to the choice of initial design point, each valid panel was optimized again with all DV values at their upper and another time with all DV values at their lower bounds. For two of the panels, when DV values were placed at their minimums (and thus creating initially

infeasible designs), the optimizer was unable to converge to an optimal solution. However, for all remaining cases, the optimization results were not significantly different.

Panel S16 converged in four iterations to a final weight of 373 kg (823 lb), which only represents a 1% weight savings over the initial design with component thickness values given in Table 2 and component weights in Table 5. The maximum deflection occurred in the upper deck surface under the right tire of the traffic load while maximum Tsai-Wu failure criterion occurred in the longitudinal stiffener at the left edge of the panel. Panel S8 converged in five design cycles to a final weight of 245 kg (540 lb) (3% weight savings). Maximum deflection occurred in the upper face plate due to the right tire of the traffic load, while the maximum Tsai-Wu failure criterion occurred in the transverse stiffener that directly connects to the simply-supported longitudinal stiffener at the edge of the panel. Panel S5 converged to 216 kg (477 lb) (5% weight savings) in ten design iterations. Maximum deflection occurred under the right tire of the traffic load while maximum Tsai-Wu failure criterion occurred at the connection of the transverse stiffener that was directly under the right tire and the simply-supported longitudinal stiffener at the right edge of the panel. Panel S3 reached convergence in eight iterations with a final weight of 212 kg (468 lb) (1% weight savings). The maximum deflection occurred under the right tire while maximum Tsai-Wu failure criterion occurred at the connection of a transverse stiffener that carried a portion of the right tire and the simply-supported longitudinal stiffener at the right edge of the panel. Panel SD3 converged to a final panel weight of 111 kg (245 lb), representing a 55% weight savings. For this panel, both the longitudinal and transverse stiffeners ply thickness constraints were active in the final design. Maximum deflection occurred under the right tire while maximum Tsai-Wu failure criterion occurred at the connection of a transverse

stiffener that carried a portion of the right tire and the simply-supported longitudinal stiffener at the right edge of the panel, similar to S3.

Assuming a 5.1 cm (2 in) asphalt wearing surface and rounding final ply thicknesses upwards to fabrication precision, the final total weight of the lightest panel, SD3, is 788.3 kg (1738 lb), in comparison to an equivalent minimum-thickness reinforced-concrete deck of 2540 kg (5600 lb). This design met AASHTO strength design requirements as well as the probabilistic deflection constraints of β=4.6 (for L/180) and β=-0.5 (for =L/360) over a 75-year design lifespan.

Design Variable Sensitivities

Figure 7 illustrates the normalized sensitivity of the reliability index (β) constraint with respect to design variables for all five optimized panel concepts, which is numerically calculated as the change in reliability index with respect to design variable value. From the plot it can be seen that the upper face plate ply thickness dominates the design sensitivities as expected. Another trend is the decreasing importance of the stiffener ply thickness and the lower face plate ply thickness as the number of stiffeners is decreased. Thus, S3 and SD3 show the highest sensitivity to stiffener thickness, especially the longitudinal stiffeners. The lower face plate ply thickness also increases in importance as more stiffeners are added.

Random Variable Sensitivities

For each of the panels, sensitivities of the random variables are numerically calculated as the change in reliability index (β) with respect to the mean (μ) and standard deviation (σ) of each random variable. Normalized plots of random variable sensitivities are presented in Figure 7 for panel SD3, which are nearly identical for all the panel concepts. The results show that live

load (LL) has the most influence on reliability index. Of secondary importance are the impact load (IM) and component thickness values of the longitudinal stiffeners (LST), transverse stiffeners (TST), upper face plate (UFT), and lower face plate (LFT). The longitudinal Young's modulus for the four components (i.e., LSE1, TSE1, UFE1, LFE1) also has some influence. The remaining random variables, shear modulus (G) and transverse Young's modulus (E2) have little significance and might be removed from future reliability efforts for problems of this type to reduce computational effort. Comparing one model to the next, it appears that the importance of the upper face plate thickness (UFT) increases as the number of stiffeners decreases. This effect was expected and is similar to the design variable sensitivities in this regard.

Summary and Conclusions

A reliability-based optimization (RBO) procedure was developed and applied to minimize the weight of fiber-reinforced polymer (FRP) composite bridge deck panels subject to probabilistic deflection and deterministic strength constraints. The presented procedure allows the use of independent optimization, finite element, and reliability analysis codes. All bridge deck panel concepts optimized converged to final weights that were less than initial, traditionally-designed structures.

The best design had 37 stiffeners in each direction (spacing of 6.774 cm (2.667 in)), with 17.8 cm (7 in) deep stiffeners. The design was governed by local deck surface deflection under the wheel load, which was best addressed with closely-spaced stiffeners and a relatively high stiffness to strength ratio as compared to the other panels. The final weight of this design with a 5.1 cm (2 in) asphalt overlay was 68% lighter than a comparable reinforced concrete bridge deck designed per AASHTO code. If only the weight of the bridge deck panel is considered, there is

a 95% weight savings over a comparable reinforced concrete bridge deck. The optimization procedure itself presented an approximately 55% weight savings compared to the same FRP deck design using conventional means. Of course, the amount of weight savings will vary depending on the types of constraints imposed on the design.

The reliability-based optimization problems explored here were relatively simple in that only four design variables and eighteen random variables were included. This is not a limitation of the methodology, but rather of the computational costs. This reduced problem required considerable computational effort, and it is recommended that future work in this area be directed toward reducing these costs. Such a reduction may also allow the inclusion of additional design options, such as shape optimization, multiple reliability constraints, instability constraint, as well as the potential for system reliability analysis.

References

American Association of State Highway and Transportation Officials (AASHTO). (2004). *AASHTO LRFD bridge design specifications*. 3rd Ed., Washington, D.C.

Antonio, C.A.C., Soeiro, A.V., and Marques, A.T. (1993). "Optimization in reliability based design of laminated composite structures." *International Conference on Computer Aided Optimum Design of Structures, Computer Aided Optimum Design of Structures III: Optimization of Structural Systems and Applications*, Zaragoza, Spain, 391-400.

Aref, A.J., Parsons, I.D., and White, S. (1999)."Manufacture, design, and performance of a modular fiber reinforced plastic bridge." Proceedings of the 31st International SAMPE Technical Conference (Edited by J.E. Green and D.D. Howell). Chicago, IL, U.S., SAMPE, v 31, 581-591.

Bakeri, P. A. (1989). "Analysis and design of polymer composite bridge decks." *Master's Thesis*, Massachusetts Institute of Technology, Cambridge, U.S.

Bakeri, P. A., and Sunder, S. S. (1990). "Concepts for hybrid FRP bridge deck systems." *Serviceability and Durability of Construction Materials, Proceedings of the 1st Materials Engineering Congress*, Denver, Colorado, U.S., ASCE, 1006-1015.

Conceicao Antonio, C. A. (2001). "A hierarchical genetic algorithm for reliability-based design of geometrically non-linear composite structures." *Composite Structures*, v 54, n 1, 37-47.

Deo, S. K. and Rais-Rohani, M. (1999). "Reliability-based design of composite sandwich plates with non-uniform boundary conditions." *40th AIAA/ASME/ASCE/AHS/ASC Structures, Structural Dynamic, and Materials Conference*, St. Louis, MO, U.S., AIAA paper 99-1580.

DOT – Design Optimization Tools Users Manual (v 5.0). (1999). Vanderplaats Research and Development, Inc., Colorado Springs, CO, U.S.

Feng, Y.S. and Song, B. F. (1990). “Reliability analysis and design for multi-box structures.” *Computers and Structures*, v 37, n 4, 413-422.

Fletcher, R. and Reeves, R. M. (1964). Function Minimization by Conjugate Gradients. The Computer Journal, 7, 149-160.

Frangopol, D. (1997). "How to incorporate reliability in structural optimization." *Chapter 11 in ASCE Manual on Engineering Practice No. 90: Guide to Structural Optimization* (Edited by J. S. Arora), 211-235.

GangaRao, H.V.S., and Laosiriphone, K. (2001). “Design and construction of market street bridge—WV.”*46th International SAMPE Symposium and Exhibition (Proceedings)*, v 46 II, 1321-1330.

Gillespie, J.W., Eckell, D.A., Edberg, W.M., Sabol, S.A., Mertz, D.R., Chajes, M.J., Shenton III, H.W., Hu, C., Chaudhri, M., Faqiri, A., and Soneji, J. (2000). “Bridge 1-351 over muddy run: Design, testing and erection of an all-composite bridge.” *Transportation Research Record*, v 2, n 1696, 118-123.

He, Y. and Aref, A. J. (2003). “An optimization design procedure for fiber reinforced polymer web-core sandwich bridge deck systems.” *Composite Structures*, v 60, iss. 2, 183-195.

Henry, J.A. (1985). “Deck-girder systems for highway bridges using fiber reinforced plastics.” *M.S. Thesis*, North Carolina State University, Raleigh, U.S.

Jones, R. M. (1999). *Mechanics of Composite Materials*. Taylor and Francis, 2nd Ed. London.

Kogiso, N. and Nakagawa, S. (2003). “Lamination parameters applied to reliability-based in-plane strength design of composites.” *AIAA Journal*, v 41, n 11, 2200-2207.

Kumar, P., Chandrashekhara, K., and Nanni, A.(2004). “Structural Performance of a FRP Bridge Deck,” Construction and Building Materials, v 18, n 1, 35-47.

Liu, X. and Mahadevan, S. (1996). "Reliability-based optimization of composite structures." *Probabilistic Mechanics and Structural Reliability, Proceedings of the Seventh Specialty Conference*, Worcester, MA, U.S., ASCE, 122-125.

Lopez-Anido, R., GangaRao, V. S., and Barbero, E. (1997). "FRP modular system for bridge decks." *Building to Last; Proceedings of Structures Congress XV*, Portland, Oregon, U.S., ASCE, 1489-1493.

McGhee, K. K., Barton, F. W., and McKeel, W. T. (1991) "Optimum design of composite bridge deck panels." *Advanced Composites Materials in Civil Engineering Structures, Proceedings of the Specialty Conference*, Las Vegas, Nevada, U.S. ASCE, 360-370.

Mertz, D. R., Chajes, M.J., Gillespie, J.W., Kukich, D.S., Sabol, S.A., Hawkins, N.M, Aquino, W., and Deen, T.B. (2003). "Application of fiber reinforced polymer composites to highway infrastructure." *National Cooperative Highway Research Program Report 503*. Transportation Research Board, Washington, D.C.

Miki, M., Murotsu, Y., Tanaka, T., and Shao, S. (1997). "Reliability-based optimization of fibrous laminated composites." *Reliability Engineering and System Safety*, v 56, iss 3, 285-290.

MIL-17 Composite Materials Handbook. (1999). Materials Sciences Corp., University of Delaware, and Army Research Laboratory.

Mosallam, A., Haroun, M., Kreiner, J., Dumlao, C., and Abdi, F. (2002). "Structural evaluation of all-composite deck for Schuyler Heim Bridge." *47th International SAMPE Symposium and Exhibition (Proceedings)*,v 47 I, 667-679.

MSC/NASTRAN Quick Reference Guide (v 70.5). (1998). MacNeal-Schwendler Corp., Los Angeles, CA, U.S.

Nowak, A. S. (1999). "Calibration of LRFD Bridge Design Code." *National Cooperative Highway Research Program Report 386*. Transportation Research Board, Washington, D.C.

Nowak, A.S. and Kim, S. (1998). "Development of a Guide for Evaluation of Existing Bridges, Part I." UMCEE 98-12, University of Michigan, March 1998.

Nowak, A.S., Sanli, A., and Eom, J. (1999). "Development of a Guide for Evaluation of Existing Bridges, Part II." UMCEE 99-13, University of Michigan, December.

Plecnick, J., Azar, W., and Kabbara, B. (1990). "Composite applications in highway bridges." *Serviceability and Durability of Construction Materials, Proceedings of the 1st Materials Engineering Congress*, Denver, Colorado, U.S., ASCE, 986-995.

Rackwitz, R. and Fiessler, B. (1978) "Structural Reliability Under Combined Random Load Sequence," *Computers and Structures,* No. 9.

Rais-Rohani, M., and Singh, M. N. (2004). "Comparison of global and local response surface techniques in reliability-based optimization of composite structures." *Journal of Structural and Multidisciplinary Optimization* (in press), v 26, n 5, 333-345.

Richard, F., and Perreux, D. (2000). "Reliability method for optimization of [+φ, -φ] fiber reinforced composite pipes." *Reliability Engineering and System Safety*, v 68, n 1, 53-59.

Riha, D. S., Thacker, B.H., Hall, D.A., Auel, T.R., and Pritchard, S.D. (1999). "Capabilities and applications of probabilistic methods in finite element analysis." *Fifth ISSAT International Conference on Reliability and Quality in Design*, Las Vegas, Nevada, U.S., August 11-13. International Society of Science and Applied Technologies.

Stoll, F., Klosterman, D, Gregory, M., Banerjee, R., Campell, S., and Day, S. (2002). "Design,

fabrication, testing, and installation of a low-profile composite bridge deck." Proceedings of the 47th International SAMPE Symposium & Exhibition, Long Beach, CA, U.S. SAMPE.

Su, B., Rais-Rohani, M., and Singh, M. N. (2002). "Reliability-based optimization of anisotropic cylindrical shells with response surface approximations of buckling instability." *43rd AIAA/ASME/ASCE/AHS/ASC Structures, Structural Dynamic, and Materials Conference*, Denver, CO, U.S., AIAA paper 2002-1386.

Vanderplaats, G.N. (1983). A Robust Feasible Directions Algorithm for Design Synthesis. Proceedings of the 24th AIAA/ASME/ASCE/AHS Structures, Structural Dynamics and Materials Conference, Lake Tahoe, Nevada, May 2-4, 1983.

VisualDOC How To Manual (v 3.0). (2002). Vanderplaats Research and Development, Inc., Colorado Springs, CO, U.S.

Williams, B., Shehata, E., and Rizkalla, S. H. (2003). "Filament-wound glass fiber reinforced polymer bridge deck modules." *Journal of Composites for Construction*, v 7, iss 3, 266-273.

Wu, Y.-T., Millwater, H. R., and Cruse, T. A. (1990). "Advanced probabilistic structural analysis method for implicit performance functions." *AIAA Journal*, v 28, n 9, 1663-1669.

Yang, L. and Ma, Z. K. (1990). "Optimum design based on reliability for a composite structural system." *Computers and Structures*, v 36, n 5, 785-790.

Zureick, A., Shih, B., and Munley, E. (1995). "Fiber-reinforced polymeric bridge decks." *Structural Engineering Review*, v 7, n 3, 257-266.

Zureick, A. (1997). "Fiber-reinforced polymeric bridge decks." *Proceedings of the National Seminar on Advanced Composite Material Bridge*, Arlington, Virginia, Federal Highway Administration.

List of Tables

List of Figures

Table 1 – Material Properties of S2-449 43.5k/SP 381 Unidirectional Glass-Epoxy Tape

Material Property	Symbol	Mean Value	Standard Deviation
Longitudinal Young's modulus	E_1	47.6 GPa	2.38 GPa
Transverse Young's modulus	E_2	13.3 GPa	0.665 GPa
Shear modulus	G_{12}	4.75 GPa	0.238 GPa
Poisson's ratio	ν_{12}	0.28	0.014
Longitudinal dir. ply tensile strength	X_T	1700 MPa	119 MPa
Longitudinal dir. ply comp. strength	X_C	1160 MPa	127 MPa
Transverse dir. ply tensile strength	Y_T	62.1 MPa	3.11 MPa
Transverse dir. ply comp. strength	Y_C	197 MPa	9.83 MPa
Ply in-plane shear strength	S	98.6 MPa	4.93 MPa
Material density	ρ	1.85 g/cm^3	N/A

Table 2 – RBO Results: Initial and Final Component Thicknesses

Layout	Upper face plate thickness (cm)		Lower face plate thickness (cm)		Long. stiff. thickness (cm)		Trans. stiff. thickness (cm)	
	Initial	Final	Initial	Final	Initial	Final	Initial	Final
S3	1.016	0.9796	0.508	0.5027	0.163	0.1445	0.163	0.1185
S5	0.935	0.9163	0.467	0.4883	0.406	0.3458	0.406	0.2936
S8	1.138	1.1175	0.467	0.5255	0.488	0.4620	0.488	0.5054
S16	2.261	2.1348	0.531	0.5819	0.983	1.0459	0.983	1.0642
SD3	0.122	0.3729	0.061	0.2011	0.406	0.0813	0.406	0.0813

Table 3 – Statistical Parameters of Random Variables

RV*	Mean	COV	Standard Deviation	Distribution
LL_{wheel}	776.8 kPa	0.13	101 kPa	Lognormal
IM_{wheel}	256.3 kPa	0.80	205.1 kPa	Ext. Type I
Ply t_i	Vary	0.01	Vary	Normal
E_{1i}	47642.8 MPa	0.05	2382.1 MPa	Weibull**
E_{2i}	13306.9 MPa	0.05	665.3 MPa	Weibull**
G_{12i}	4750.5 KPa	0.05	237.5 KPa	Weibull**

*i=1-4 for a total of 18 RVs.
**The use of a normal distribution did not alter results.

Table 4 – Results for Reliability Calibration

Layout	β L/360	β L/180	β Strength
S3	-0.422	4.595	10+
S5	-0.497	4.705	10+
S8	-0.551	4.651	10+
S16	-0.550	4.617	10+
SD3	-0.551	4.557	3.4

Table 5: RBO Results: Component Weights

Layout	Total Weight (kg)		Upper face plate (kg)		Lower face plate (kg)		Stiffeners (kg)	
	Initial	Final	Initial	Final	Initial	Final	Initial	Final
S3	215	213	105	108	52	55	58	50
S5	228	217	100	100	50	54	78	63
S8	253	245	131	123	54	58	68	64
S16	378	374	249	234	59	64	70	76
SD3	247	111	6	41	3	22	102	48

Table 6 – Analysis Information

Layout	No. of Optimization Cycles	Total CPU Time, hrs
S3	8	79.2
S5	10	52.0
S8	5	18.7
S16	4	7.0
SD3	4	39.7

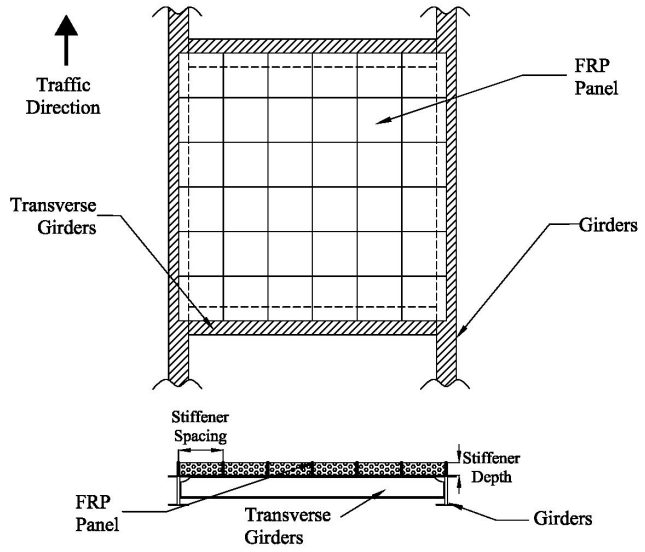

Figure 1 - Bridge Deck Panel

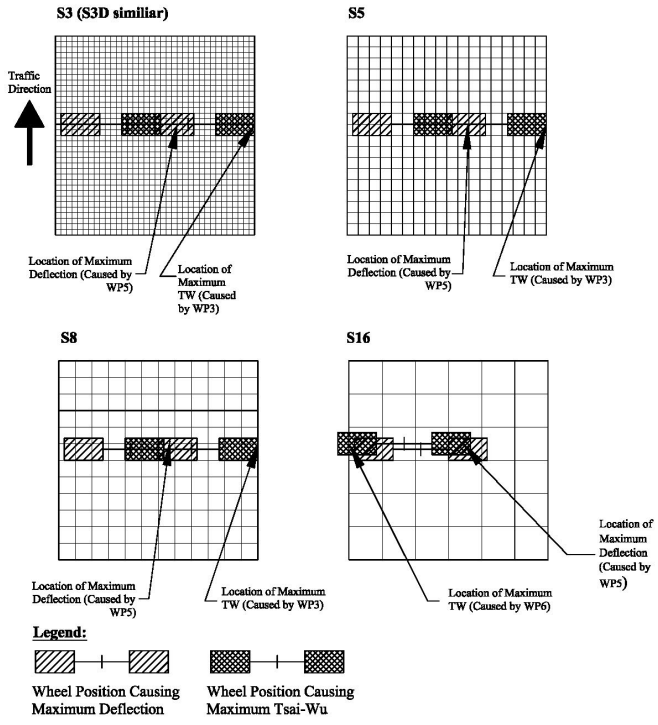

Figure 2 - Wheel Positions and Locations of Maximum Deflection and Stress

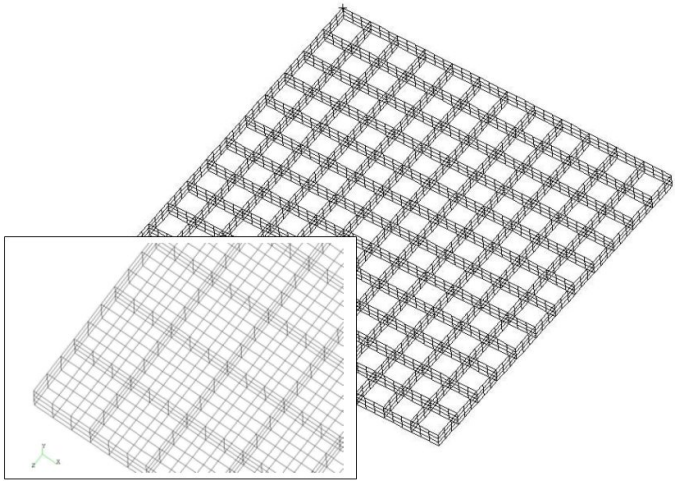

Figure 3 - Finite element model of S8 (top of deck surface removed for clarity)

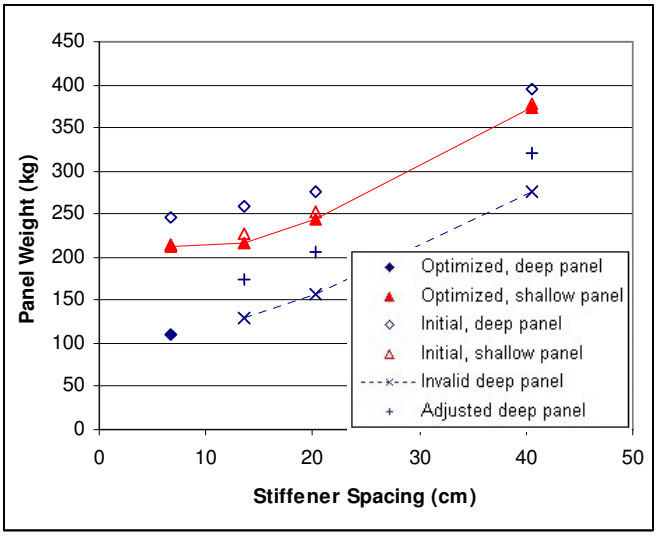

Figure 4 - Final Results of RBO

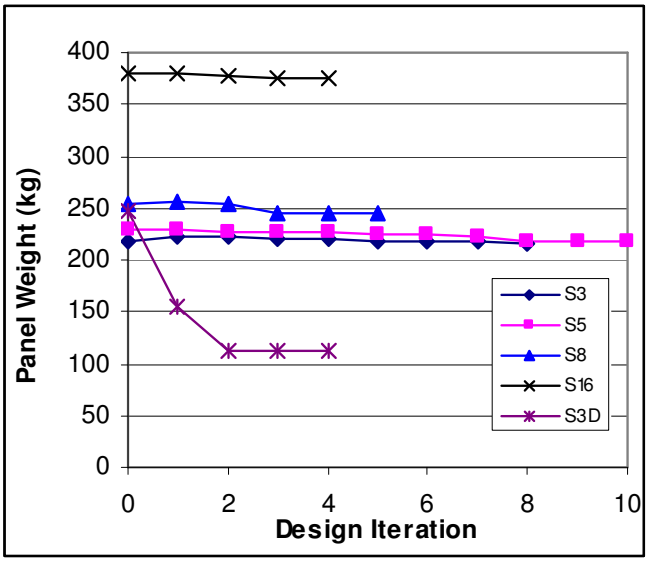

Figure 5 - Objective function history for 5 RBO models

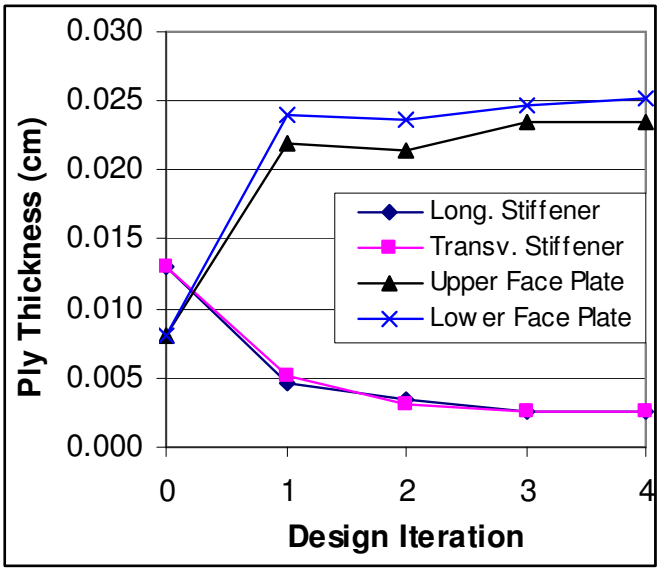

Figure 6 - Design variable changes for SD3

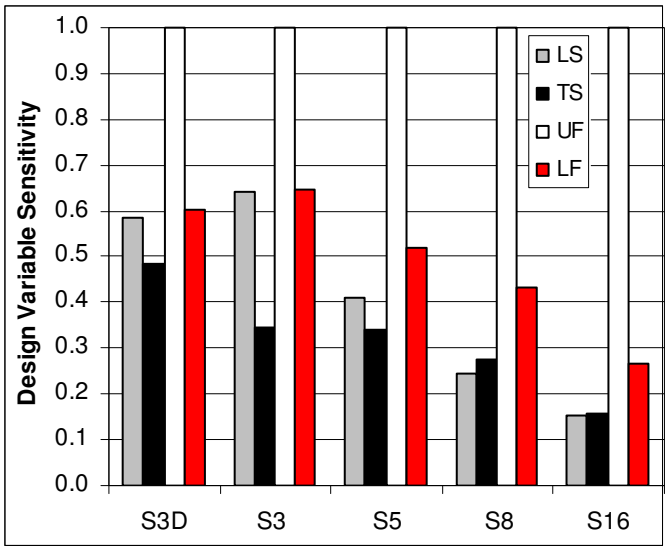

Figure 7 – β Constraint sensitivities of design variables

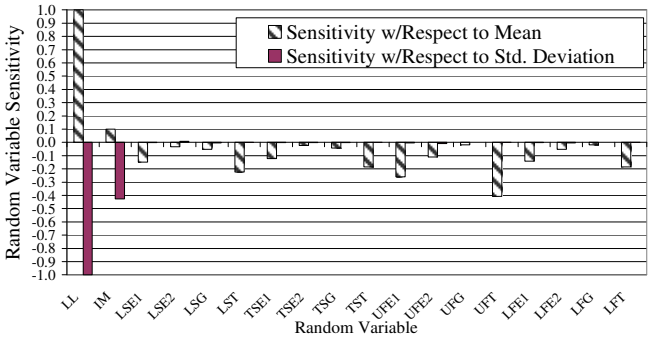

Figure 8 - Random Variable Sensitivity factors for SD3